

PIXELS TO INSIGHTS: DEEP LEARNING FOR FLOODWATER DEPTH MAPPING IN SETTLEMENT AREAS.

Jeffrey Blay, Leila Hashemi-Beni

College of Science and Technology, North Carolina A&T State University, Greensboro, NC-USA

jblay@aggies.ncat.edu, lhashemibeni@ncat.edu

Abstract: This study maps the maximum floodwater depth in Kinston, North Carolina, using high-resolution aerial imagery and LiDAR data for Hurricane Matthew. A UNET regression model with a ResNet-18 backbone was employed to predict floodwater depth by integrating extracted floodwater extent boundaries and corresponding terrain data (Digital Elevation Models) based on physical principles. Model training utilized 6,322 patches comprising floodwater extent boundaries, DEMs, and ground truth depth masks. The trained model achieved a Root Mean Squared Error (RMSE) of approximately 0.11. When tested on two study areas, the model predicted maximum floodwater depths of 4.8 ft and 4.7 ft for Test Areas 1 and 2, respectively. These results demonstrate the model's potential for accurate floodwater depth prediction and applicability to initiatives to mitigate flood impacts in urban settlements.

Keywords: Flood Depth, LiDAR, Aerial imagery, U-net, Artificial intelligence.

I. INTRODUCTION

Populated areas face significant risks from severe and frequent flooding, leading to substantial loss of life and property damage. The growing flood risks in these areas are primarily driven by climatic and socio-economic factors, including the increasing population in flood-prone areas. Climatic changes, combined with human-induced socio-economic dynamics, exacerbate flood hazards. Human activities, such as land-use changes and CO₂ emissions, further influence the hydrodynamic processes of flooding in vulnerable regions [1]. Over the past two decades, global flood events have risen by approximately 40% and continue to increase, with projections indicating that 68% of new floods will be driven by tides and storm events [2], [3].

In the United States, Hurricane Matthew (2016) resulted in 49 fatalities and an estimated economic loss of \$13 billion across multiple states [4]. North Carolina was the most severely impacted state, experiencing significant property damage and loss of life. Reports indicate that the hurricane claimed the lives of 32 individuals in the state and caused an economic loss of approximately \$ 2 billion. This included damage to around 110,000 physical structures (homes and businesses) and business interruptions [5]. For decision makers to mitigate the impacts of floods, it is crucial to

accurately map the dynamics of flooding to inform effective initiatives.

High-resolution remote sensing data, combined with advanced data engineering techniques, have become essential in environmental phenomena, particularly flood analysis. These approaches have been widely applied to flood extent and depth mapping in urban areas [6], as well as other environmental applications such as landslides mapping [7], water quality [8], [9], precision agriculture [10], and wetland mapping [11]. For instance, [12] used a Convolutional Neural Network (CNN) and fine-resolution rainfall hyetograph data to predict real-time pluvial and fluvial urban flood extent and depth. Similarly, [13] applied an enhanced ResNet50 model and urban waterlogging data from social media to estimate urban flood depth levels. [14] leveraged multiple machine learning algorithms and rainfall patterns to predict urban flood inundation. These modern approaches are gaining popularity in literature due to the limitations of traditional methods, such as manual observation, sensor monitoring, and hydrodynamic models. Conventional methods often face challenges like data scarcity, limited spatial coverage, and time-intensive processes.

This study contributes to advancing emerging techniques for urban flood mapping by leveraging high-resolution remote sensing data to train a CNN algorithm for predicting floodwater depth. The study specifically emphasizes urban floodwater depth prediction, providing vital insights for the development and implementation of sustainable flood mitigating initiatives.

II. DATA AND METHODOLOGY

This study utilizes the UNET algorithm to estimate floodwater depth from Hurricane Matthew in Kinston, North Carolina. High-resolution aerial imagery and LiDAR data serve as the primary datasets for this research. The remainder of this section is structured as follows: study area, the datasets description and preprocessing, and model training.

A. Study Area

Kinston is a city in Lenoir County, North Carolina, USA, with a population estimate of 19,411 [15]. The city is located along the Neuse River basin. During Hurricane Matthew, the Neuse river reached a peak level of 28.31 feet, following approximately 16.5 inches of rainfall [5], [16]. This event caused significant damage to life and property within the city. Two study sites were selected from the city

for this study (Fig. 1). They both cover a total land area of approximately 715 (Table 1) acres along the Neuse River.

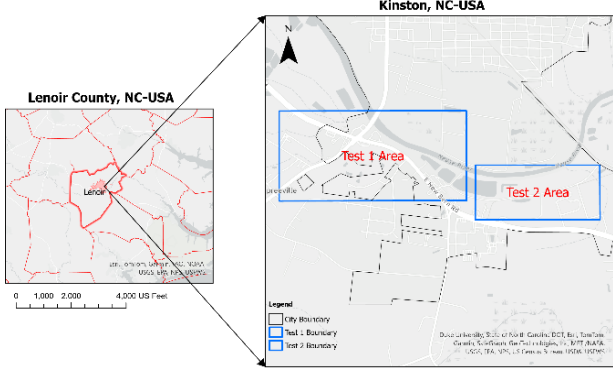


Fig. 1. Study area map- Kinston

Table 1: Total land area for each study area

Study Area	Land area (acres)
Test Area 1	507.87
Test Area 2	207.49

B. Dataset Description and Pre-processing

This study utilized high-resolution post-flood aerial imagery from Hurricane Matthew, obtained through the [NOAA Storm Archive](#), and high resolution LiDAR data from North Carolina emergency management ([NC SDD](#)), were acquired for this study. The aerial imagery has a spatial resolution of 0.25 meters, while the LiDAR data features a density of two points per meter (0.5-meter spatial resolution). These datasets were acquired for three training sites affected by Hurricane Matthew in North Carolina: Lumberton, Goldsboro, and Princeville (Fig. 2).

The aerial imagery was used to estimate floodwater extent boundaries, while the LiDAR data was employed to generate terrain data in the form of Digital Elevation Models (DEMs). Following the approach implemented in [6], [17], a pre-trained UNET model was used to extract floodwater extent boundaries from the high-resolution imagery for each site. Digital Elevation Models were created from the LiDAR dataset by extracting the ground points and applying linear interpolation, resulting in a high-resolution 0.5-meter DEM raster for each site. To ensure spatial coherence with the terrain data, the imagery was resampled to 0.5 meters prior to floodwater boundary extraction. Ground truth floodwater depth estimations were manually derived by integrating the extracted flood extent boundaries with the generated DEMs, based on established physical principles and methodologies outlined in [18], [19].

Subsequently, 256 x 256 patches were generated for the floodwater extent boundaries, the corresponding DEMs, and the ground truth floodwater depth mask for each study site (Fig. 3). Floodwater depth prediction is treated as an image-to-image translation task, with both input and output as raster

data. Processing the input data into smaller patches, rather than entire catchment areas, ensures sufficient diverse training data, improving model generalization [20]. In total, 6,322 patches were created to train and test the UNET algorithm for floodwater depth prediction. The 6,322 patches were split into training and testing datasets, with 80% (5057) used for training and 20% (1265) reserved for testing. This split ensured sufficient data for model evaluation while preventing overfitting by using a separate testing set to evaluate the model's performance.

The patches were further processed to simplify and enhance model training for improved prediction and generalization. Specifically, the DEM and ground truth depth patches were normalized using the min-max normalization technique, which reduced variability in pixel values across the different training sites. Additionally, the DEM patches were concatenated with the water extent boundary patches to form the input X for the model (Fig. 3). This approach aligns with the physical principle that floodwater extent and terrain data (DEM) are essential for accurately predicting floodwater depth.

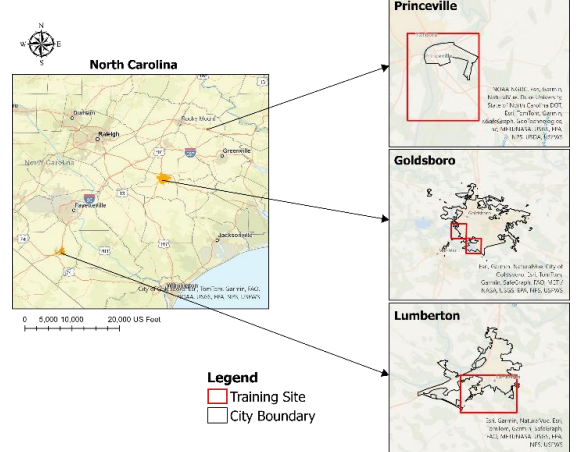


Fig. 2. Training Sites for data collection

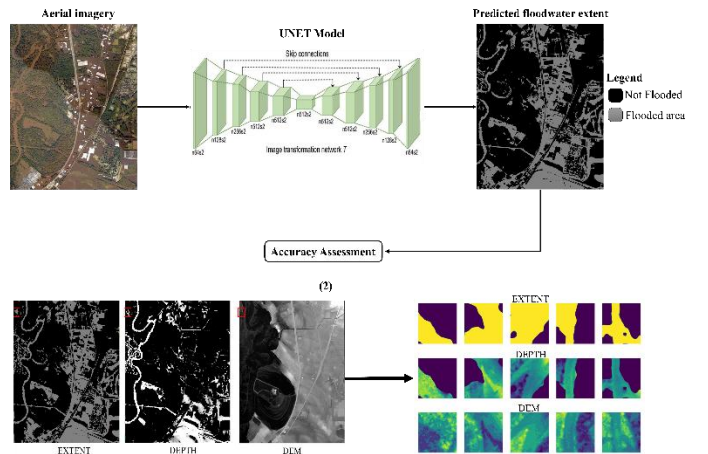


Fig. 3. Datasets description and processing

C. Model Architecture

The UNET regression model integrated with the ResNet-18 architecture was utilized for this study. The ResNet-18 model addresses the challenges of vanishing and exploding gradients in deep networks by introducing residual learning through skip connections, which allow the direct passage of input to output. This facilitates network optimization and supports the effective training of deeper architectures [21].

The ResNet-18 architecture comprises 18 layers, including the input layer, residual blocks, batch normalization, ReLU activation functions, pooling layers, and a fully connected layer [21] (Fig. 4).

D. Model Training

The model was trained with the following hyperparameters: a fixed learning rate of 0.0001, a batch size of 8, and 40 epochs. A linear activation function was used for the output. This is essentially suited for floodwater depth prediction, as it allows the model to predict continuous range of values. Also, a custom Root Mean Squared Error (RMSE) loss function was implemented, which was specifically designed to ignore non-flooded areas in the prediction. This was important to focus the model's learning on the flood-affected regions to improve accuracy (Fig. 4).

The model was trained without encoder weights to allow the model to learn floodwater-specific features from scratch and enhance the model's ability to predict unseen data, rather than generalized features suited for other image classification tasks. After the training, the results were evaluated using the RMSE metric. The implementation was carried out using TensorFlow 2.10 in Python.

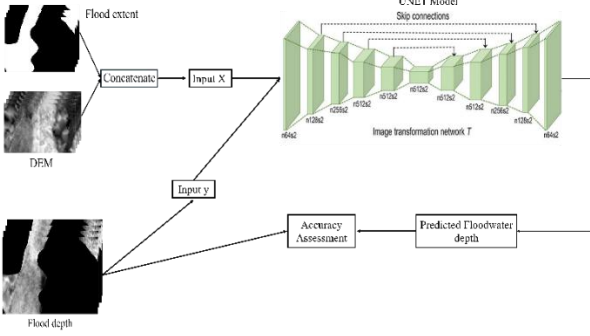


Fig. 4. Resnet 18 U-net model training process

III. RESULTS AND DISCUSSION

The results of this study highlight the importance of accurate flood extent boundaries and high-resolution DEM data in enhancing model training and predictive performance for floodwater depth estimation [22]. The flood extent boundary, derived from high-resolution aerial imagery, demonstrated an accuracy of approximately 97%, significantly contributing to the training data's reliability [6]. The model exhibited consistent learning across epochs, with steadily decreasing training and validation losses, indicating

effective optimization and reduced overfitting (Fig. 5). With an RMSE of approximately 0.11, the model showcased its ability to predict floodwater depths with minimal deviation approximately of 0.1ft from ground truth measurements, affirming its robustness on unseen data. Predictions for Test Area 1 revealed a maximum floodwater depth of 4.8 ft and a minimum of 2.5 ft, while Test Area 2 showed a maximum of 4.7 ft and a minimum of 0.01 ft, which closely aligned with observed data (Fig. 6). These findings underscore the model's potential for practical applications in flood impact assessment and mitigation planning in urban areas.

Building on these results, the study demonstrates the critical role of integrating high-resolution datasets with advanced deep learning networks for maximum floodwater depth prediction. The combination of floodwater extent boundaries and terrain data not only aligns with hydrological principles but also emphasizes the potential of leveraging data-driven approaches to complement hydrodynamic models [12], [20], [23]. The detailed predictions of maximum and minimum floodwater depths across the test areas offer actionable insights, which could be pivotal for urban flood management strategies, including evacuation planning and infrastructure resilience analysis.

Despite the performance of the model, significant steps could be taken to further refine the predictions. Future works could explore the incorporation of additional datasets, such as land-use characteristics, as well as rainfall intensity (for studies looking at the temporal dynamics of floods). Also, key terrain indicators such as aspect, curvature, and slope could be incorporated to improve floodwater depth prediction accuracy. Additionally, testing this approach against other extreme flood events could also enhance the model's reliability for decision-making in disaster risk management.

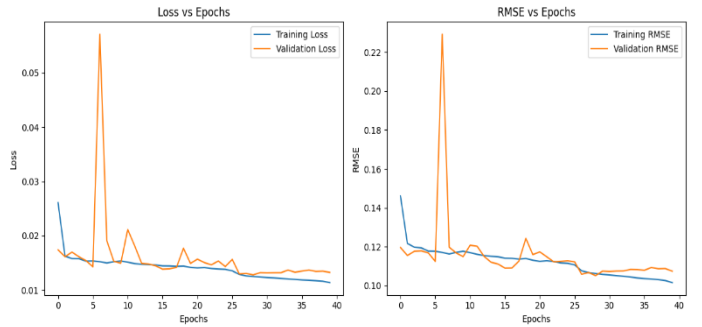


Fig. 5. Model training plot.

IV. CONCLUSION

This study demonstrated the effectiveness of combining high-resolution aerial imagery and LiDAR-derived DEMs with a ResNet18-UNet model to predict floodwater depth. By integrating floodwater extent boundaries and terrain data, the model achieved a low RMSE of 0.11 and accurately predicted floodwater depths across study areas. These results provide valuable insights for flood risk management and planning in urban areas. It also highlights the significant benefit of multi-data fusion in

remote sensing studies[24]. Future work could explore applying this approach to other regions and incorporating more data to improve accuracy and usability. Furthermore, integrating physics-informed knowledge, as proposed in [25], could improve model training and lead to more robust results.

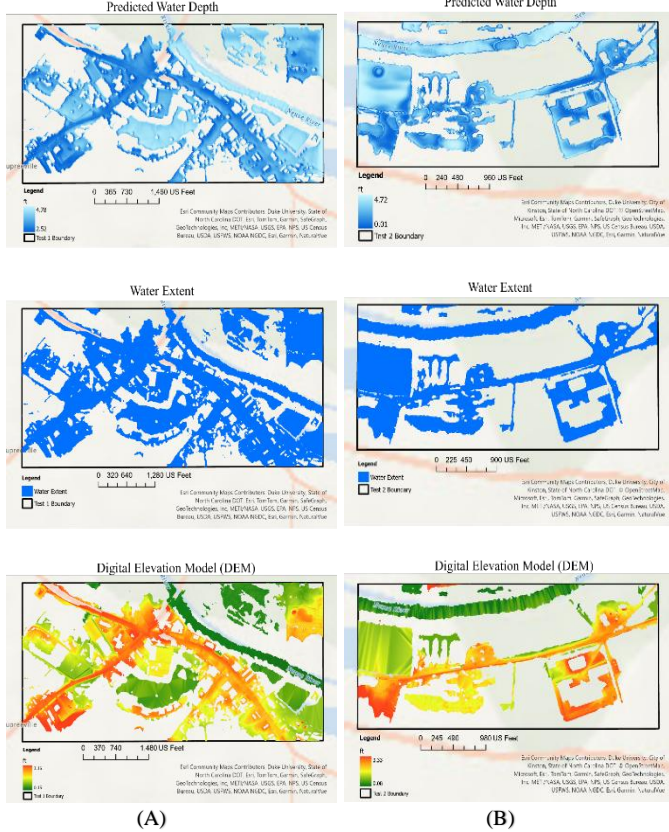


Fig. 6. (A) Floodwater depth prediction with corresponding extent boundary and DEM for Test area 1. (B) Floodwater depth prediction with corresponding extent boundary and DEM for Test area 2.

V. ACKNOWLEDGMENT

This work is supported by NASA award 80NSSC23M0051 and NSF award 2401942.

VI. REFERENCES

- [1] E. Ridolfi, E. Mondino, and G. Di Baldassarre, "Hydrological risk: modeling flood memory and human proximity to rivers," *Hydrology Research*, vol. 52, no. 1, pp. 241–252, Feb. 2021, doi: 10.2166/nh.2020.195.
- [2] K. J. Wienhold, D. Li, W. Li, and Z. N. Fang, "Flood Inundation and Depth Mapping Using Unmanned Aerial Vehicles Combined with High-Resolution Multispectral Imagery," *Hydrology*, vol. 10, no. 8, p. 158, Jul. 2023, doi: 10.3390/hydrology10080158.
- [3] M. Fereshtehpour, M. Esmailzadeh, R. S. Alipour, and S. J. Burian, "Impacts of DEM type and resolution on deep learning-based flood inundation mapping," *Earth Sci Inform*, vol. 17, no. 2, pp. 1125–1145, Apr. 2024, doi: 10.1007/s12145-024-01239-0.
- [4] NOAA National Centers for Environmental Information (NCEI), "U.S. Billion-Dollar weather and Climate Disasters," National Centers for Environmental Information -NOAA. Accessed: Jan. 05, 2025. [Online]. Available: <https://www.ncei.noaa.gov/access/billions/>
- [5] A. Benfield, "Hurricane Matthew Event Recap Report." Apr. 2017. Accessed: Oct. 30, 2024. [Online]. Available: https://www.actuarialpost.co.uk/downloads/cat_1/Aon-hurricane-matthew-recap.pdf
- [6] J. Blay, M. Fawakherji, and L. Hashemi-Beni, "Flood impact risk mapping in settlement areas from a 3D perspective: A case study of hurricane matthew," presented at the 2024 IEEE International Geoscience and Remote Sensing Symposium, Athens, Greece: IEEE, Sep. 2024. doi: 10.1109/IGARSS53475.2024.10640634.
- [7] G. Agboola, L. H. Beni, T. Elbayoumi, and G. Thompson, "Optimizing landslide susceptibility mapping using machine learning and geospatial techniques," *Ecological Informatics*, vol. 81, p. 102583, Jul. 2024, doi: 10.1016/j.ecoinf.2024.102583.
- [8] E. T. Wasehun, L. H. Beni, C. A. Di Vittorio, C. M. Zarzar, and K. R. L. Young, "Comparative analysis of Sentinel-2 and PlanetScope imagery for chlorophyll-a prediction using machine learning models," *Ecological Informatics*, vol. 85, p. 102988, Mar. 2025, doi: 10.1016/j.ecoinf.2024.102988.
- [9] L. Hashemi-Beni, M. Puthenparampil, and A. Jamali, "A low-cost IoT-based deep learning method of water gauge measurement for flood monitoring," *Geomatics, Natural Hazards and Risk*, vol. 15, no. 1, p. 2364777, Dec. 2024, doi: 10.1080/19475705.2024.2364777.
- [10] F. Dorbu and L. Hashemi-Beni, "Detection of Individual Corn Crop and Canopy Delineation from Unmanned Aerial Vehicle Imagery," *Remote Sensing*, vol. 16, no. 14, p. 2679, Jul. 2024, doi: 10.3390/rs16142679.
- [11] M. Anokye, M. Fawakherji, and L. Hashemi-Beni, "Flood Resilience Through Advanced Wetland Prediction," in *IGARSS 2024 - 2024 IEEE International Geoscience and Remote Sensing Symposium*, Athens, Greece: IEEE, Jul. 2024, pp. 5516–5520. doi: 10.1109/IGARSS53475.2024.10641585.
- [12] M. El Baida, F. Boushaba, M. Chourak, and M. Hosni, "Real-Time Urban Flood Depth Mapping: Convolutional Neural Networks for Pluvial and Fluvial Flood Emulation," *Water Resour Manage*, May 2024, doi: 10.1007/s11269-024-03886-w.
- [13] L. Wu *et al.*, "Identification of flood depth levels in urban waterlogging disaster caused by rainstorm

- using a CBAM-improved ResNet50,” *Expert Systems with Applications*, vol. 255, p. 124382, Dec. 2024, doi: 10.1016/j.eswa.2024.124382.
- [14] G. Chen *et al.*, “Urban inundation rapid prediction method based on multi-machine learning algorithm and rain pattern analysis,” *Journal of Hydrology*, vol. 633, p. 131059, Apr. 2024, doi: 10.1016/j.jhydrol.2024.131059.
- [15] Census Bureau United States, “Quick Facts-Kinston city, North Carolina,” United States Census Bureau. Accessed: Jan. 01, 2025. [Online]. Available: <https://www.census.gov/quickfacts/fact/table/kinstoncitynorthcarolina/PST045223#PST045223>
- [16] S. Stewart, “Hurricane Matthew,” NOAA, National Hurricane Center, AL142016, Apr. 2017.
- [17] M. Fawakherji, J. Blay, M. Anokye, L. Hashemi-Beni, and J. Dorton, ‘DeepFlood for Inundated Vegetation High-Resolution Dataset for Accurate Flood Mapping and Segmentation,” *Sci Data*, vol. 12, no. 1, p. 271, Feb. 2025, doi: 10.1038/s41597-025-04554-3.
- [18] S. Cohen *et al.*, “Estimating Floodwater Depths from Flood Inundation Maps and Topography,” *J American Water Resour Assoc*, vol. 54, no. 4, pp. 847–858, Aug. 2018, doi: 10.1111/1752-1688.12609.
- [19] A. A. Gebrehiwot and L. Hashemi-Beni, “Three-Dimensional Inundation Mapping Using UAV Image Segmentation and Digital Surface Model,” *IJGI*, vol. 10, no. 3, p. 144, Mar. 2021, doi: 10.3390/ijgi10030144.
- [20] Z. Guo, J. P. Leitao, N. Simoes E., and V. Moosavi, “Data-driven flood emulation Speeding up urban flood predictions by deep.pdf.” Wiley, Nov. 18, 2020. [Online]. Available: DOI: 10.1111/jfr3.12684
- [21] K. He, X. Zhang, S. Ren, and J. Sun, “Deep Residual Learning for Image Recognition,” in *2016 IEEE Conference on Computer Vision and Pattern Recognition (CVPR)*, Las Vegas, NV, USA: IEEE, Jun. 2016, pp. 770–778. doi: 10.1109/CVPR.2016.90.
- [22] A. Gebrehiwot and L. Hashemi-Beni, “3D Inundation Mapping: A Comparison Between Deep Learning Image Classification and Geomorphic Flood Index Approaches,” *Front. Remote Sens.*, vol. 3, p. 868104, Jun. 2022, doi: 10.3389/frsen.2022.868104.
- [23] R. Löwe, J. Böhm, D. G. Jensen, J. Leandro, and S. H. Rasmussen, “U-FLOOD – Topographic deep learning for predicting urban pluvial flood water depth,” *Journal of Hydrology*, vol. 603, p. 126898, Dec. 2021, doi: 10.1016/j.jhydrol.2021.126898.
- [24] M. Fawakherji and L. Hashemi-Beni, “Flood detection and mapping through multi-resolution sensor fusion: integrating UAV optical imagery and satellite SAR data,” *Geomatics, Natural Hazards and Risk*, vol. 16, no. 1, p. 2493225, Dec. 2025, doi: 10.1080/19475705.2025.2493225.
- [25] T. Syum Gebre, L. Beni, E. Tsehay Wasehun, and F. Elikem Dorbu, “AI-Integrated Traffic Information System: A Synergistic Approach of Physics Informed Neural Network and GPT-4 for Traffic Estimation and Real-Time Assistance,” *IEEE Access*, vol. 12, pp. 65869–65882, 2024, doi: 10.1109/ACCESS.2024.3399094.